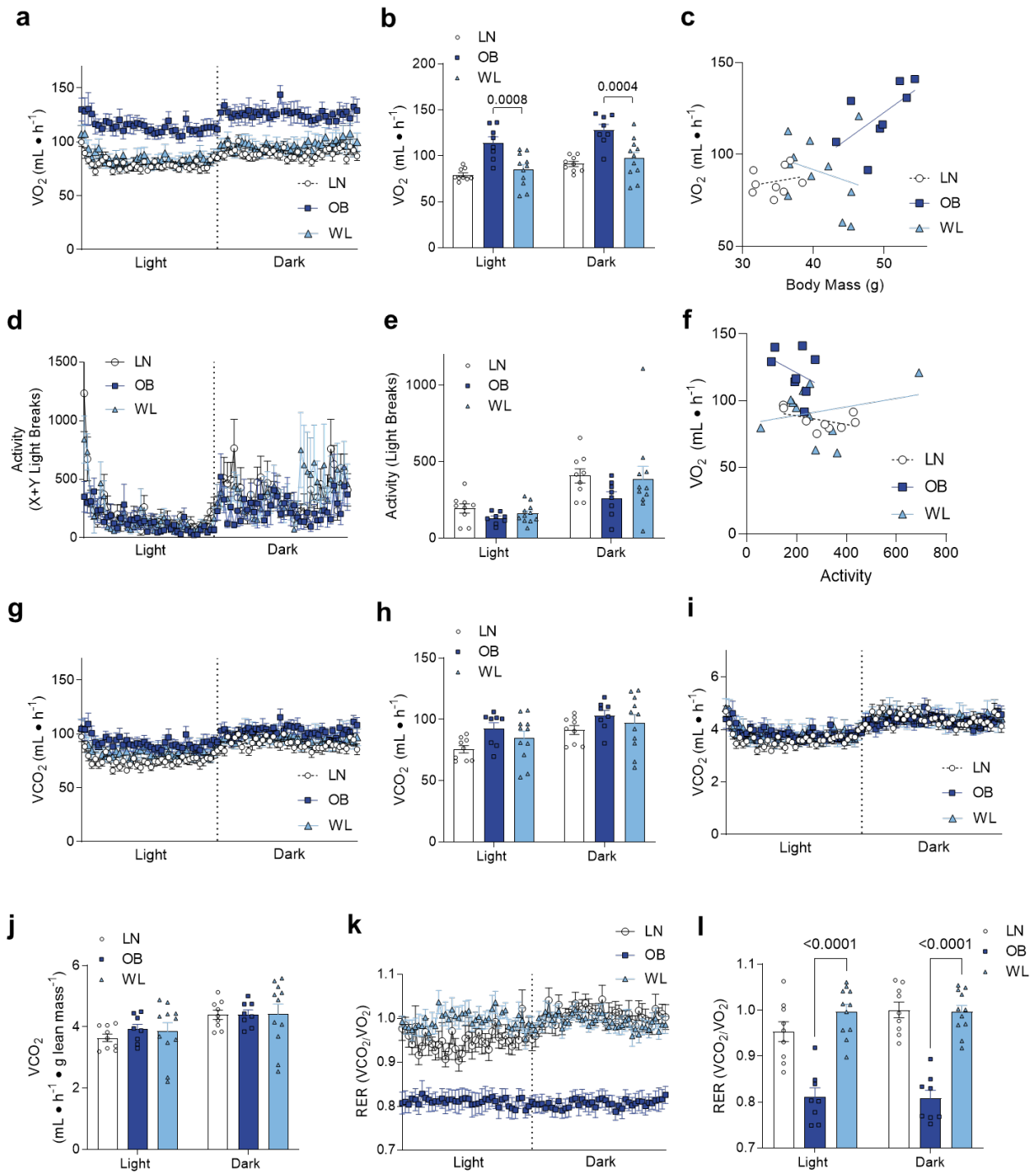


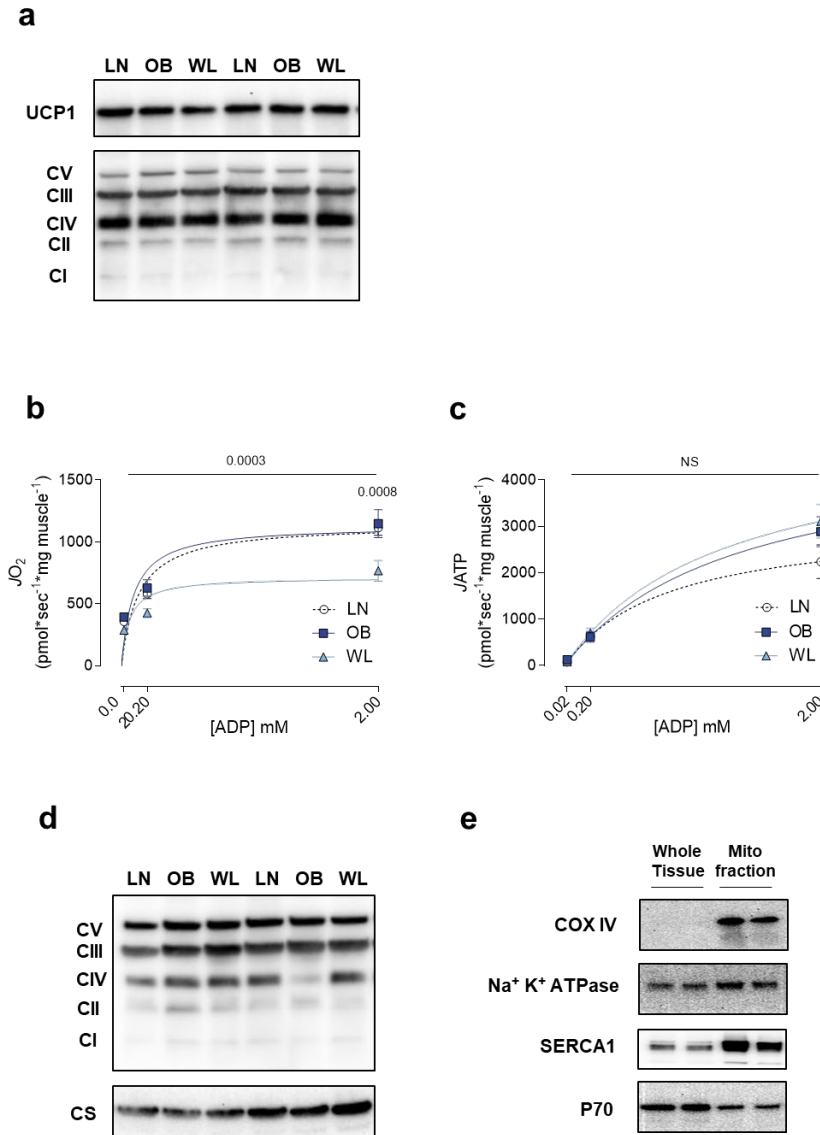
## Supplementary Figure S1



**Supplementary Figure S1.** (a&b) Total  $VO_2$  (unnormalized). (c) Relationship between body mass and total  $VO_2$  (unnormalized). (d&e) Spontaneous movement. (f) Relationship between

spontaneous movement to  $VO_2$ . (g&h) Total  $VCO_2$  (unnormalized). (i&j) Total  $VCO_2$  (normalized to lean mass). (k&l) Respiratory exchange ratio (RER).  $n=9$  for LN,  $n=8$  for OB,  $n=11$  for WL. All data are represented as mean  $\pm$  SEM. Two-way ANOVA with Sidak multiple comparisons (b,l). p-values indicate statistical significance between OB and WL groups.

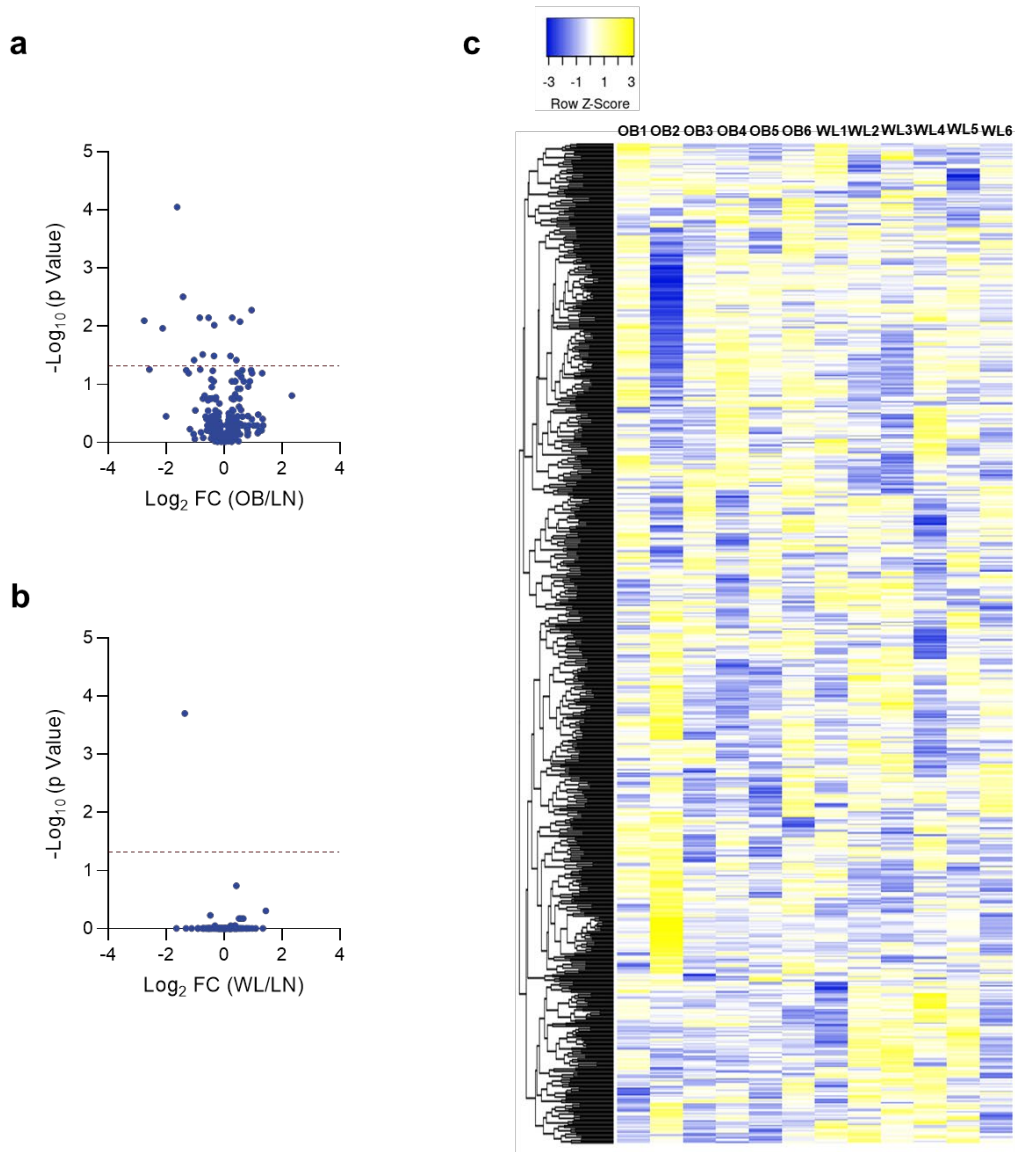
## Supplementary Figure S2



**Supplementary Figure S2.** (a) Representative western blots for OXPHOS subunits and UCP1 in homogenates from brown adipose tissues. (b) Rates for oxygen consumption ( $J_{O_2}$ ). P-value indicates statistical difference between OB and WL groups. (c) Rates for ATP production ( $J_{ATP}$ ). These numbers were used to derive Figure 2c. (d) Representative western blots for OXPHOS subunits and citrate synthase (CS) in total muscle homogenates. (e) Validation of mitochondrial enrichment in the mitochondrial fraction. Percoll gradient isolation was not

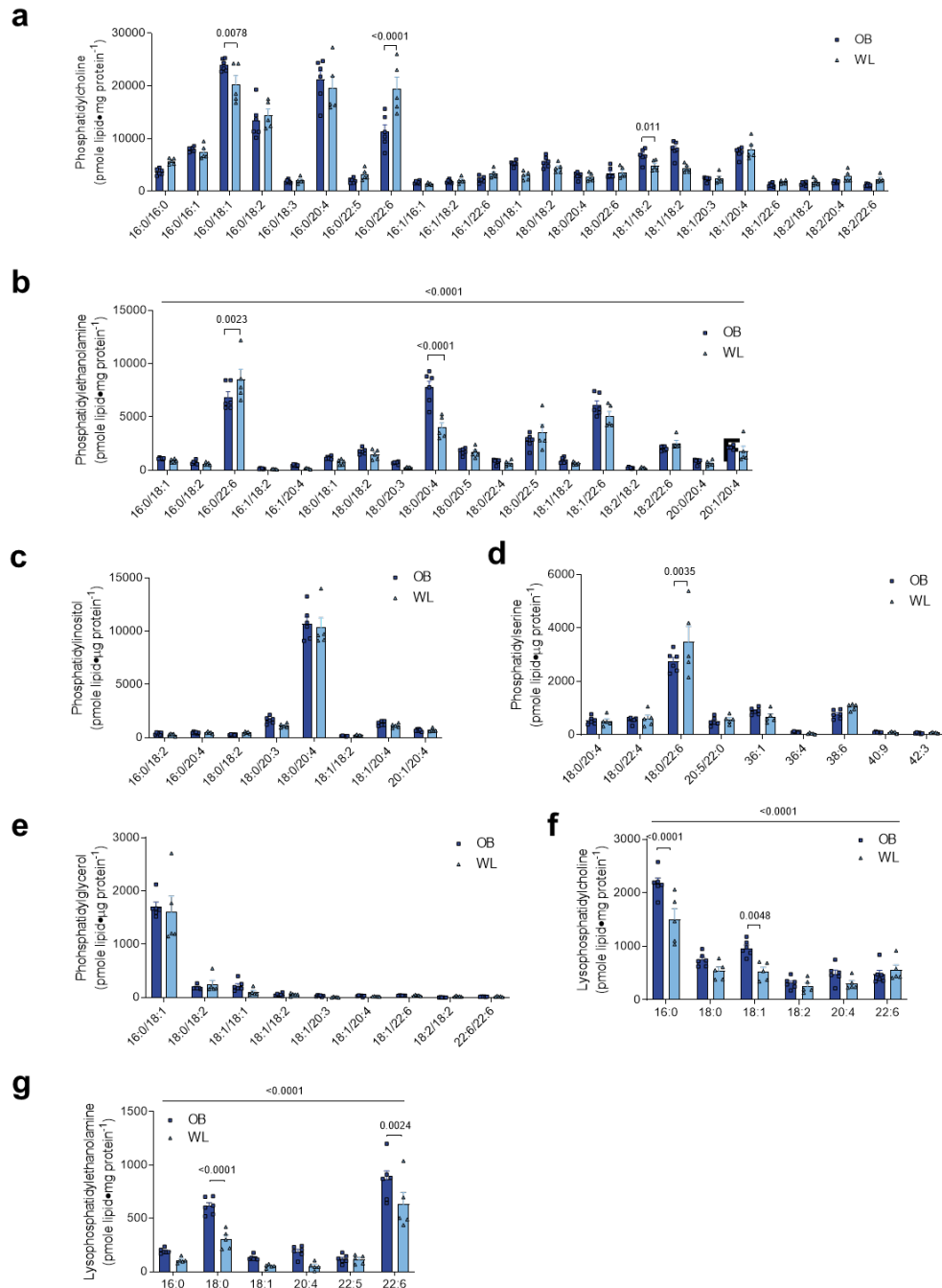
performed to preserve mitochondrial function for high-resolution respirometry and fluorometry. Blotting for mitochondrial COXIV shows that even a short exposure produces strong immunoreactivity in isolated mitochondrial fraction when such band is barely visible in whole lysate with equal protein loading. Thus, the mitochondrial fraction is highly enriched in mitochondria. In contrast, the mitochondrial fraction also includes proteins from plasma membrane (Na<sup>+</sup>/K<sup>+</sup>-ATPase), endoplasmic reticulum (SERCA), and cytosol (p70) with comparable abundance to whole lysate. Comparable enrichment of total lysate and mitochondrial prep for these organelles is likely due to myofibrillar and extracellular matrix proteins that are highly abundant in whole lysate, making it relatively dilute with intracellular organelles per µg of protein. All data are represented as mean ± SEM. Two-way ANOVA with Sidak multiple comparisons (b,c). p-values indicate statistical significance between OB and WL groups.

### Supplementary Figure S3



**Supplementary Figure S3.** (a) Volcano plot of differentially abundant mitochondria proteins between LN and OB groups. (b) Volcano plot of differentially abundant mitochondria proteins between LN and WL groups. Significance threshold shown with dotted red line for both a and b. (c) Unsupervised clustering analyses of mitochondrial proteome between OB and WL groups.

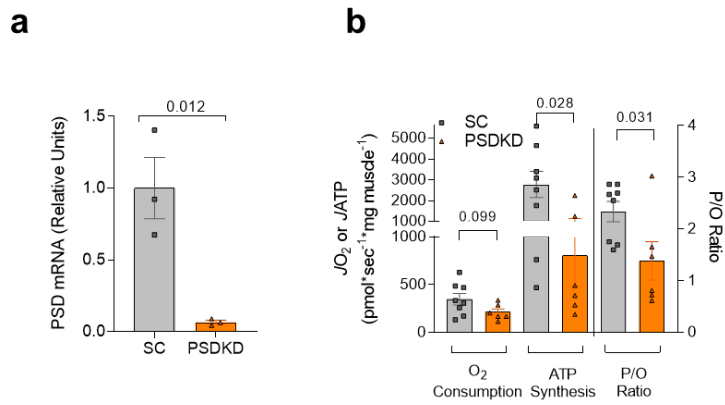
## Supplementary Figure S4



**Supplementary Figure S4.** Skeletal muscle mitochondrial lipidomic analyses. (a) Phosphatidylcholine. (b) Phosphatidylethanolamine. (c) Phosphatidylinositol. (d) Phosphatidylserine. (e) Phosphatidylglycerol. (f) Lysophosphatidylcholine. (g)

Lysophosphatidylethanolamine.  $n=6$  for OB,  $n=5$  for WL. All data are represented as mean  $\pm$  SEM. Two-way ANOVA with Sidak multiple comparisons.

## Supplementary Figure S5



**Supplementary Figure S5.** (a) PSD mRNA levels from C2C12 myotubes treated with scrambled (SC) or shPSD (PSDKD). (b) Rates for O<sub>2</sub> consumption, ATP production, and P/O ratio in isolated mitochondria from SC or PSDKD C2C12 myotubes with 200  $\mu$ M of ADP ( $n=8$  for SC,  $n=6$  for PSDKD). All data are represented as mean  $\pm$  SEM. Unpaired t-test (a,b).